



Universiteit
Leiden
The Netherlands

Crystal structures of allosamidin derivatives in complex with human macrophage chitinase

Rao, F.V.; Houston, D.R.; Boot, R.G.; Aerts, J.M.F.G.; Sakuda, S.; Aalten, D.M.F. van

Citation

Rao, F. V., Houston, D. R., Boot, R. G., Aerts, J. M. F. G., Sakuda, S., & Aalten, D. M. F. van. (2003). Crystal structures of allosamidin derivatives in complex with human macrophage chitinase. *Journal Of Biological Chemistry*, 278(22), 20110-20116. Retrieved from <https://hdl.handle.net/1887/50847>

Version: Not Applicable (or Unknown)

License:

Downloaded from: <https://hdl.handle.net/1887/50847>

Note: To cite this publication please use the final published version (if applicable).

Crystal Structures of Allosamidin Derivatives in Complex with Human Macrophage Chitinase*

Received for publication, January 13, 2003, and in revised form, March 13, 2003
Published, JBC Papers in Press, March 14, 2003, DOI 10.1074/jbc.M300362200

Francesco V. Rao^{‡§}, Douglas R. Houston^{‡§¶}, Rolf G. Boot^{||}, Johannes M. F. G. Aerts^{||},
Shohei Sakuda^{**}, and Daan M. F. van Aalten^{‡ ‡‡}

From the [‡]Division of Biological Chemistry and Molecular Microbiology, School of Life Sciences, University of Dundee, Dundee DD1 5EH, Scotland, ^{||}Department of Biochemistry, Academic Medical Center, University of Amsterdam, NL-1105 AZ Amsterdam, The Netherlands, and ^{**}Department of Applied Biological Chemistry, the University of Tokyo, Bunkyo-Ku, Tokyo 113, Japan

The pseudotrisaccharide allosamidin is a potent family 18 chitinase inhibitor with demonstrated biological activity against insects, fungi, and the *Plasmodium falciparum* life cycle. The synthesis and biological properties of several derivatives have been reported. The structural interactions of allosamidin with several family 18 chitinases have been determined by x-ray crystallography previously. Here, a high resolution structure of chitotriosidase, the human macrophage chitinase, in complex with allosamidin is presented. In addition, complexes of the allosamidin derivatives demethylallosamidin, methylallosamidin, and glucoallosamidin B are described, together with their inhibitory properties. Similar to other chitinases, inhibition of the human chitinase by allosamidin derivatives lacking a methyl group is 10-fold stronger, and smaller effects are observed for the methyl and C3 epimer derivatives. The structures explain the effects on inhibition in terms of altered hydrogen bonding and hydrophobic interactions, together with displaced water molecules. The data reported here represent a first step toward structure-based design of specific allosamidin derivatives.

Family 18 chitinases hydrolyze chitin, a polymer of β -(1,4)-linked *N*-acetylglucosamine. Chitin is not found in humans but plays a key role in the life cycles of several classes of human pathogens, such as fungi (1), nematodes (2), protozoan parasites (3), and insects (4). Several chitinase inhibitors with biological activity have been identified, such as allosamidin (5), styloguanidines (6), and the cyclic peptides CI-4 (7–9), argifin (10), and argadin (11, 12). Allosamidin (see Fig. 1) is a pseudotrisaccharide isolated from *Streptomyces* cultures (5). It consists of two *N*-acetylallosamine sugars, linked to a novel moiety termed allosamizoline, which contains a cyclopentitol group, coupled to an oxazoline that carries a dimethyl amine (Fig. 1

and Table I). The inhibitor has been shown to inhibit all family 18 chitinases, with K_i in the nM to μ M range (13, 14). It inhibits cell separation in fungi (1, 15), transmission of the malaria parasite *Plasmodium falciparum* (3, 16, 17), and insect development (13). Several natural allosamidin derivatives have been isolated and characterized (reviewed in Refs. 13 and 14), and the total synthesis of the inhibitor has been achieved through several strategies (14).

The structure of allosamidin in complex with family 18 chitinases has been solved for hevamine (18), chitinase B from *Serratia marcescens* (19), and chitinase 1 from *Coccidioides immitis* (20). A preliminary soaking study has also been reported for the human chitinase (21). The inhibitor appears to bind from the –3 to –1 subsites, with the allosamizoline occupying the –1 subsite. Several hydrogen bonds and stacking interactions with aromatic residues appear to be responsible for the tight binding of allosamidin to the family 18 chitinases (19, 20, 22). Allosamidin is thought to resemble the structure of a reaction intermediate that is unique among the glycoside hydrolases (18). Retaining glycoside hydrolases mostly function through a double displacement mechanism that involves a catalytic acid and a nucleophile and proceeds through a covalent enzyme-substrate intermediate (such as shown recently (23) for lysozyme). In family 18 chitinases, however, a suitable nucleophile is missing in the protein, and instead the reaction proceeds through nucleophilic attack of the *N*-acetyl group on the substrate itself, resulting in an oxazoline intermediate (18, 19, 24, 25) that is stabilized by the conserved Asp neighboring the catalytic Glu in the characteristic DXXDXDXE sequence motif (Fig. 2). It is this intermediate that is mimicked by allosamidin (Fig. 1). The inhibitor is hydrolytically stable, because it lacks the pyranose oxygen.

Allosamidin is a broad-spectrum inhibitor, inhibiting all characterized family 18 chitinases. If allosamidin is to be used as a pharmacophore for development of novel compounds with activity against human pathogens, it is also necessary to take into account the human macrophage chitinase identified recently (26–28). This enzyme has endochitinase activity against chitin azure and colloidal chitin (27, 29) and has been shown to be able to degrade chitin from the *Candida albicans* cell wall (29). Furthermore, 6% of the human population is homozygous for an inactivated form of the gene (26, 30), which preliminary studies have associated with an increased susceptibility to nematodal infections (31). It has therefore been proposed that the human chitinase plays a role in defense against chitinous pathogens (29, 30). Thus, it would be necessary to design allosamidin derivatives with specific activity against chitinases from pathogens but only weak inhibition of the human chitinase. Several allosamidin derivatives are already available (13,

* The costs of publication of this article were defrayed in part by the payment of page charges. This article must therefore be hereby marked "advertisement" in accordance with 18 U.S.C. Section 1734 solely to indicate this fact.

The atomic coordinates and structure factors (code 1HKK (ALLO), 1HKJ (GLCB), 1HKJ (METH), and 1HKM (DEME)) have been deposited in the Protein Data Bank, Research Collaboratory for Structural Bioinformatics, Rutgers University, New Brunswick, NJ (<http://www.rcsb.org/>).

§ Both authors contributed equally to this work.

¶ Supported by a Biotechnology and Biological Sciences Research Council CASE studentship.

‡‡ Supported by a Wellcome Trust Career Development Research Fellowship. To whom correspondence should be addressed. Tel.: 44-1382-344979; Fax: 44-1382-345764; E-mail: dava@davapcl.bioch.dundee.ac.uk.

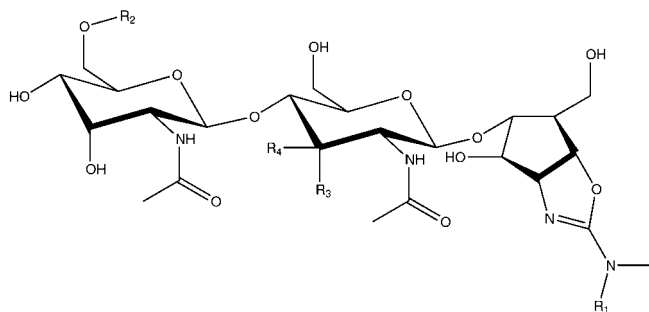


FIG. 1. **Allosamidin and its derivatives.** The two-dimensional chemical structure of the allosamidin backbone is shown. Depending on the substitutions on R_1 – R_4 the following naturally occurring derivatives are discussed in this study.

TABLE I
Substitutions of allosamidin and its derivatives

	R_1	R_2	R_3	R_4
Allosamidin (ALLO)	CH3	H	OH	H
Demethylallosamidin (DEME)	H	H	OH	H
Methylallosamidin (METH)	CH3	CH3	OH	H
Glucoallosamidin B (GLCB)	H	CH3	H	OH

14). Although complexes of family 18 chitinases with allosamidin itself have been characterized (18–20), none of its derivatives have been analyzed structurally in the context of a chitinase. As a first step toward the design of specific allosamidins, we describe here the crystal structures of the human chitinase complexed with allosamidin (ALLO)¹ and three derivatives, demethylallosamidin (DEME), methylallosamidin (METH), and glucoallosamidin B (GLCB) (Fig. 1). We also report the inhibitory properties of these derivatives against human chitinase, which, together with the structures, suggest that development of a specific, yet still potent, allosamidin-based chitinase inhibitor should be possible.

MATERIALS AND METHODS

Structure Determination—Human chitinase (HCHT) was isolated as described previously (21). As reported earlier, soaking of HCHT crystals with ALLO and its derivatives resulted in severe cracking (21). To overcome these problems, HCHT was co-crystallized with ALLO and its derivatives DEME, METH, and GLCB (Fig. 1). The complexes were formed through addition of 10 mM allosamidin derivative to the protein, which was at a concentration of 8 mg/ml. Crystals were then grown by vapor diffusion using 1 μ l of protein-inhibitor complex and 1 μ l of mother liquor consisting of 25% polyethylene glycol, 550 monomethyl ether, 0.01 M $ZnSO_4$, and 0.1 M MES, pH 6.5, equilibrated against a reservoir containing 1 ml of mother liquor. Crystals appeared after 2 days and grew to a maximum size of 0.2 \times 0.1 \times 0.1 mm. The crystals were cryoprotected in a solution of mother liquor containing 3 M Li_2SO_4 and then frozen in a nitrogen cryostream for data collection. Data were collected on beamline ID14-EH2 at the European Synchrotron Radiation Facility (Grenoble, France) and beamline X11 at the Deutsches Elektronen Synchrotron (the Deutsches Elektronen Synchrotron, Hamburg, Germany), and processed with the HKL suite of programs (32) (Table II). The HCHT·ALLO structure was solved by molecular replacement with AMoRe (33) (search model, the native HCHT structure (21); top solution, $r = 0.344$; correlation coefficient, 0.694) and was used as a starting structure for the refinement of the other complexes. Refinement was performed with CNS (34) interspersed with model building in O (35). Topologies for the allosamidins were obtained from the PRODRG server (36). The inhibitors were not included until defined by unbiased $|F_o| - |F_c|$, ϕ_{calc} maps (Fig. 3).

Enzymology—The IC_{50} values (*i.e.* inhibitor concentration resulting

in 50% inhibition) of the allosamidin derivatives were determined using the fluorogenic substrate 4-methylumbelliferyl- β -D-*N,N,N'*-triaceetylchitotriose (4MU-NAG₃; Sigma) in a standard assay, as described previously (26). Briefly, in a final volume of 125 μ l, a constant amount of enzyme was incubated with 0.022 mM substrate in McIlvain buffer (100 mM citric acid, 200 mM sodium phosphate, pH 5.2) containing 1 mg/ml bovine serum albumin, for 20 min at 37 $^{\circ}C$ in the presence of different concentrations of inhibitor. After addition of 2.5 ml of 0.3 M glycine-NaOH, pH 10.6, the fluorescence of the liberated 4MU was quantified using a PerkinElmer Life Sciences LS2 fluorimeter (excitation 445 nm, emission 366 nm). The ability of chitotriosidase to transglycosylate does not allow determination of K_i values.

RESULTS AND DISCUSSION

Overall Structures—HCHT were grown in the presence of ALLO, DEME, METH, and GLCB (Fig. 1). The crystals diffracted to 1.85, 2.55, 2.60, and 2.55 \AA , respectively. The structures were solved by molecular replacement using the native HCHT structure as a search model (21) and refined to R-factors (R_{free}) of 0.181 (0.192), 0.215 (0.257), 0.211 (0.253), and 0.225 (0.275), respectively. Models for the allosamidins were only included in the refinement, when they were well defined by unbiased $F_o - F_c$, ϕ_{calc} density (Fig. 3). Analysis of Ramachandran plots calculated with PROCHECK (37) reveal that there is only one residue (Asp-328) in a disallowed conformation, yet electron density for this residue is well defined.

The allosamidins bind in a groove on the chitinase, occupying subsites -3 to -1 (Figs. 3 and 4). In the HCHT·ALLO complex, a second, disordered, allosamidin molecule (average B-factors 40.1 \AA^2 , compared with 20.8 \AA^2 for the first molecule) is observed to bind to the protein, approximately occupying the $+1$ to $+3$ subsites. It is possible that this represents a weaker binding interaction and only occurs because of the high concentrations (10 mM) of allosamidin in the mother liquor. Subsequent comparisons and discussions will focus on the ordered allosamidin molecule only.

Three chitinase-allosamidin complexes have been reported previously for hevamine (18), chitinase B from *S. marcescens* (19), and chitinase 1 from *C. immitis* (20). In the HCHT·ALLO structure, the inhibitor binds in the same location and orientation as observed in these complexes. There are no significant backbone conformational changes; the HCHT·ALLO complex superimposes with an root mean square deviation of 0.36 \AA on the HCHT structure C α atoms. The tightest interactions are formed with the allosamizoline in the -1 subsite, which is lined with residues that are conserved in family 18 chitinases from a wide range of organisms (Figs. 2 and 3). Trp-358 stacks with the hydrophobic face of the allosamizoline, similar to the interaction of this residue with the -1 boat pyranose in the chitinase B-NAG₅ complex (19). Tyr-27, Phe-58, Gly-98, Ala-183, Met-210, and Met-356 are the main contributors to a hydrophobic pocket, which is occupied by the two allosamizoline methyl groups (Figs. 3 and 4). The allosamizoline moiety has several hydrogen bonding interactions with the protein (see Table IV). Asp-138 stabilizes the positive charge on the oxazoline (Fig. 3) and is flipped $\sim 180^{\circ}$ around χ_1 compared with the native structure (21), as also observed in all other chitinase·ALLO complexes (19, 20, 22). The backbone nitrogen of Trp-99 hydrogen bonds the allosamizoline O3 (Fig. 3). On the opposite side of the inhibitor, Tyr-212 and Asp-213 hydrogen bond with the allosamizoline O7 and O6, respectively (Fig. 3).

In the chitinase B·ALLO structure, an ordered water molecule was observed within 3.3 \AA of the allosamizoline C1 carbon, and subsequent analysis of the hevamine·ALLO complex also revealed such a water molecule (19). A similar water molecule is also found upon inspection of the *C. immitis* CTS1·ALLO complex published recently (20). This interaction is thought to be reminiscent of the attack of a water molecule, which hydrolyzes the oxazolinium ion reaction intermediate (19). However,

¹ The abbreviations used are: ALLO, allosamidin; DEME, demethylallosamidin; METH, methylallosamidin; GLCB, glucoallosamidin B; HCHT, human chitinase; MES, 4-morpholineethanesulfonic acid.

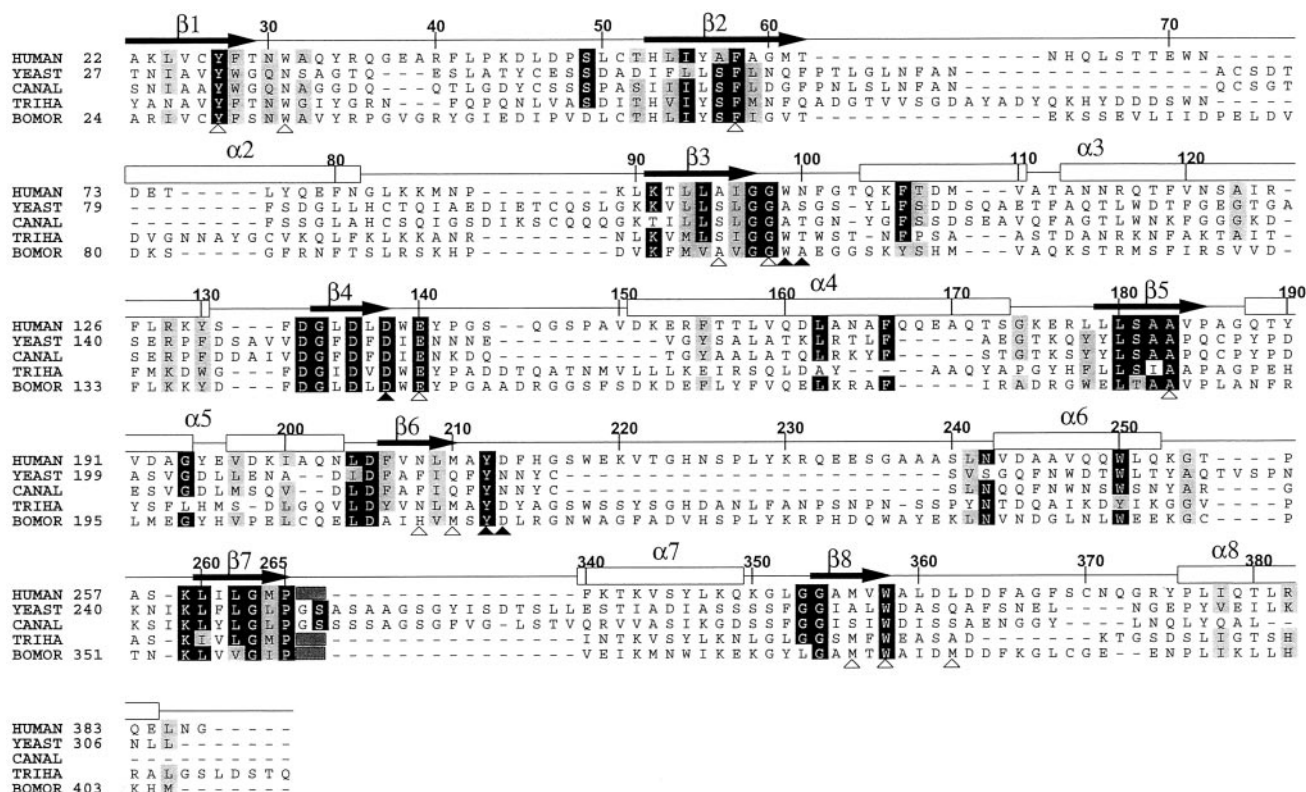


FIG. 2. Multiple sequence alignment of chitinases. Sequences of the human chitinase (HUMAN), *S. cerevisiae* CTS1 (YEAST), *C. albicans* chitinases (consensus sequence; CANAL), *T. harzianum* chitinases (consensus sequence; TRIHA), and *B. mori* chitinase (BOMOR) were aligned with T-coffee (41) and shaded with BOXSHADE. Numbering and secondary structure is according to the human chitinase. Triangles indicate residues that form mainly hydrophobic (open) or hydrogen bonding (filled) interactions with allosamidin in the HCHT·ALLO complex (see also Fig. 3). The human, *T. harzianum*, and *B. mori* chitinases possess an extra α/β domain that is represented in the alignment by a gray box (after residue 265 for HCHT). This domain is absent in the *S. cerevisiae* and *C. albicans* chitinases.

TABLE II
Details of data collection and structure refinement

Values in parentheses are for the highest resolution shell. Crystals were of space group $P4_32_12$ and were cryo-cooled to 100 K. All measured data were included in structure refinement.

	ALLO	DEME	METH	GLCB
Cell dimensions (Å)	$a = 94.86$ $b = 94.86$ $c = 83.48$	$a = 93.83$ $b = 93.83$ $c = 86.90$	$a = 93.99$ $b = 93.99$ $c = 87.09$	$a = 94.14$ $b = 94.14$ $c = 88.43$
Resolution range (Å)	25–1.85 (2.92–1.85)	25–2.55 (2.64–2.55)	25–2.60 (2.69–2.60)	25–2.55
No. observed reflections	201273 (13633)	63006 (6132)	54650 (5358)	52134 (5376)
No. unique reflections	32893 (3050)	13215 (1283)	12526 (1233)	13275 (1306)
Redundancy	6.1 (4.5)	4.8 (4.8)	4.4 (4.3)	3.9 (4.1)
$I/\sigma I$	15.9 (5.2)	11.3 (2.3)	11.4 (2.5)	11.3 (2.7)
Completeness (%)	99.3 (93.8)	99.6 (98.9)	99.9 (100.0)	98.7 (100.0)
R_{sym} (%)	4.8 (31.4)	10.3 (64.2)	9.4 (64.5)	8.3 (66.1)
R_{crys} (%)	18.1	21.5	21.1	22.5
R_{freel} (%)	19.2	25.7	25.3	27.5
No. R_{freel} reflections	675	260	246	261
No. protein atoms	2871	2877	2877	2877
No. water molecules	253	53	48	66
No. inhibitor atoms	86	42	44	43
Root mean square deviation from ideal geometry				
Bonds (Å)	0.010	0.008	0.011	0.012
Angles (°)	2.0	1.4	1.6	1.9
B-factor Root mean square deviation (Å ²) (bonded, main chain)	1.4	1.5	1.5	1.6
B_{protein} (Å ²)	27.4	42.9	44.3	46.7
$B_{\text{inhibitor}}$ (Å ²)	30.5	31.7	33.8	44.9

this water molecule is not observed in the complexes with the allosamidins described here. In the HCHT·ALLO complex, the position of this water molecule is occupied by the *N*-acetyl group of the second disordered allosamidin molecule. The relatively low resolution diffraction data for the complexes with the allosamidin derivatives may not be sufficient to define the position of this particular water molecule.

Although the allosamidin moiety tightly binds conserved residues through hydrogen bonding and hydrophobic interactions, there are fewer interactions with the two *N*-acetylallosamine sugars in the -2 and -3 subsites (see Table IV). The sugar in the -2 subsite makes two hydrogen bonds to Asn-100, via the O4 and O6 atoms (Fig. 3). Further hydrogen bonds are formed from O3 to Glu-297 and from Trp-358 to O7. The methyl

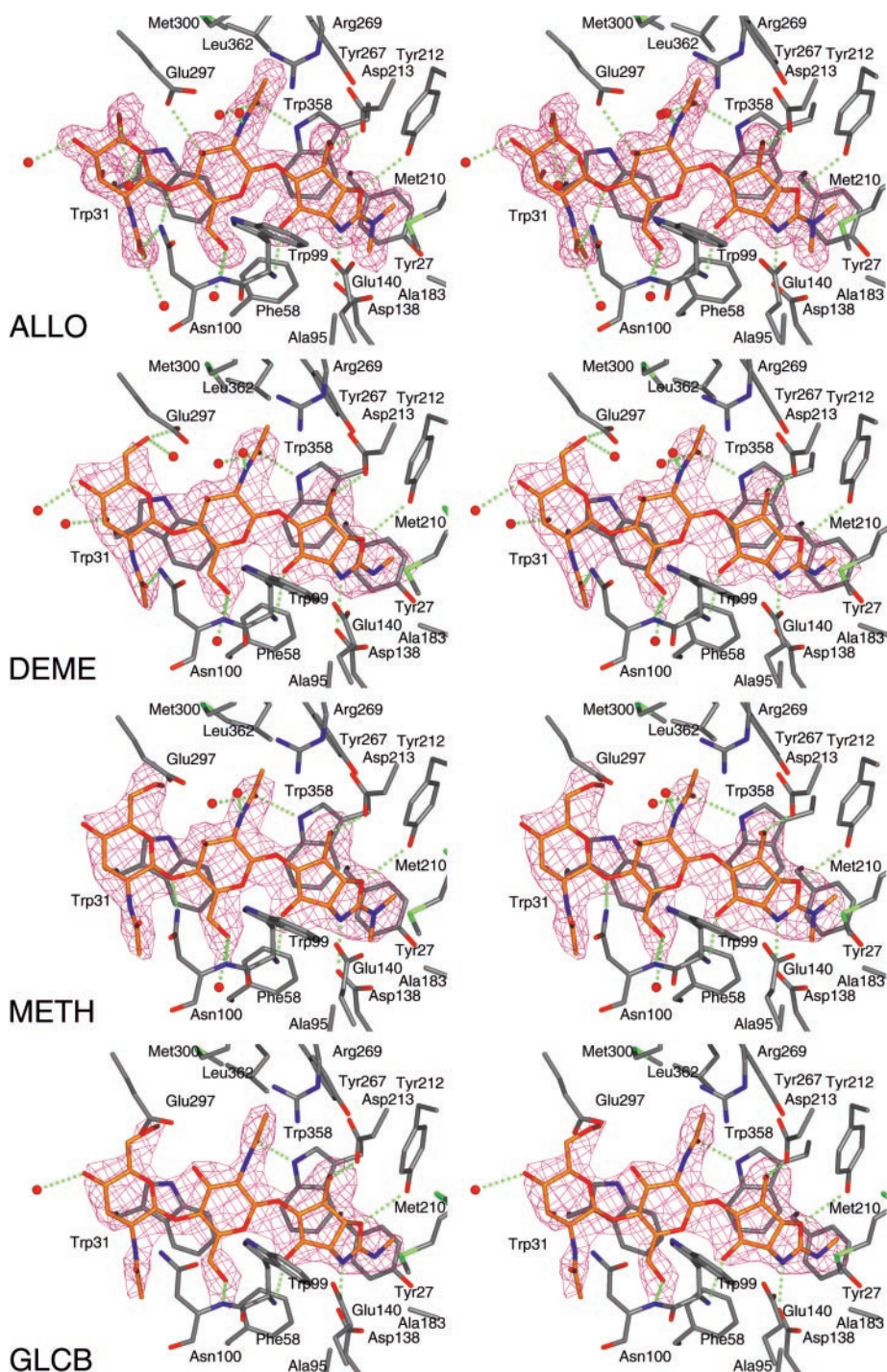


FIG. 3. Complexes with allosamidin derivatives. Stereo images of the final structures of the human chitinase in complex with allosamidin and its derivatives are shown. Side chains interacting with the allosamidins (also indicated in Fig. 2) are shown in a sticks representation. The allosamidins are shown as a sticks model with orange carbons. Water molecules involved in allosamidin hydrogen bonds are shown as red spheres. Hydrogen bonds are shown as dotted green lines and are listed in Table IV. The unbiased $F_o - F_c, \phi_{\text{calc}}$ maps before inclusion of models for the inhibitors in the refinement are shown in magenta, contoured at 2.25σ .

on the *N*-acetyl group binds in a hydrophobic pocket formed by Tyr-267, Met-300, and Leu-362 (Fig. 3). The -3 sugar stacks with Trp-31, whereas a hydrogen bond is formed with the side chain of Glu-297 (Fig. 3). Two ordered water molecules mediate several inhibitor-protein hydrogen bonds (Fig. 3). Residues 266–337 form the α/β domain in HCHT, which is absent in the smaller family 18 chitinases such as hevamine and the fungal chitinases (Figs. 2 and 4). Therefore, these smaller enzymes have a more solvent exposed -2 subsite and almost no interactions with the *N*-acetylallosamine at -3 (18).

Enzymology—A large number of allosamidin derivatives have been synthesized and characterized for their biological activity (reviewed in Refs. 13 and 14). Here, we have focused on three derivatives (DEME, METH, and GLCB; Fig. 1) for which enzymological data with several chitinases is already available

(compiled in Ref. 13) (Table III). We have determined the apparent IC_{50} values of these derivatives against human chitinase using a standard assay with the fluorescent substrate 4-methylumbelliferyl-chitotriose (4MU-NAG₃) (Table III). The IC_{50} for ALLO (40 nM) has been reported previously (38). Removal of one of the methyl groups on the allosamizoline moiety leads to an ~ 20 -fold increase in affinity (DEME; Fig. 1), compared with ALLO. If an extra methyl group is added to the O6 hydroxyl on the -3 allosamine, a similar increase in inhibition is observed (METH; Fig. 1 and Table III). If both these modifications are combined together with epimerization at carbon C3, only a 5-fold stronger inhibition is measured (GLCB; Fig. 1 and Table III), compared with ALLO. These data (together with other demethylallosamidin derivatives not discussed here (13)) suggest that the major effect on inhibition is the large increase

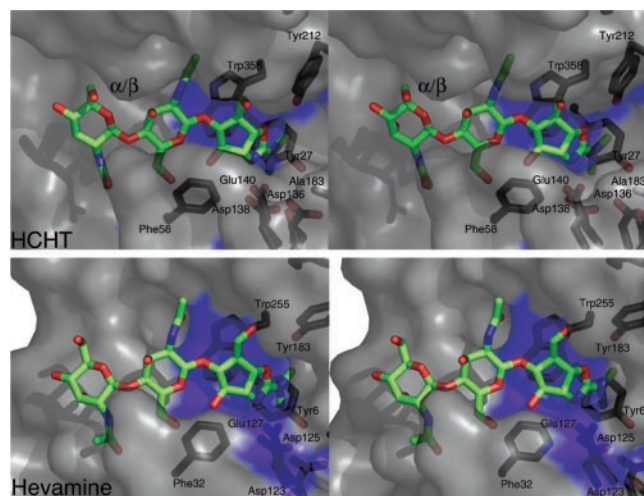


FIG. 4. **Sequence conservation in the active site.** Stereo image of the molecular surfaces calculated from HCHT in the HCHT·ALLO complex and hevamine in the hevamine·ALLO complex (18) is shown. Blue surface corresponds to conserved residues (Fig. 2), which are also shown as a sticks model. ALLO is shown as a sticks model with green carbons. The $\alpha\beta$ domain, absent in hevamine, is indicated in HCHT.

TABLE III
Apparent IC_{50} values of the allosamidin derivatives against chitinases from different species

IC_{50} values of human chitinase were determined by variation of inhibitor concentrations. Assays were performed as described under "Materials and Methods." All constants are expressed in nM. IC_{50} values for *S. cerevisiae*, *C. albicans*, *T. harzianum*, and *B. mori* were taken from Ref. 13.

	<i>S. cerevisiae</i>	<i>C. albicans</i>	<i>T. harzianum</i>	<i>B. mori</i>	Human
ALLO	55000	10000	1300	48	40
DEME	480	1100	1300	81	1.9
METH	60000	14000	1900	65	2.6
GLCB	810	1300	2600	65	8.0

TABLE IV
HCHT-inhibitor hydrogen bonds

Hydrogen bonds between the protein and inhibitor were calculated with WHAT IF (39) using the HB2 algorithm (40). This algorithm gives a 0 (no hydrogen bond) to 1 (optimal hydrogen bond) score to reflect hydrogen bond geometry (40) (HB2 column). A cut-off of 0.3 was applied here to exclude weak hydrogen bonds. Inhibitor hydrogen bonding potential was calculated with PRODRG (36). Donor acceptor distances in Å are also listed (D-A).

Atom	-1 subsite			-2 subsite			-3 subsite		
	Protein/water	D-A	HB2	Protein/water	D-A	HB2	Protein/water	D-A	HB2
N2 ALLO	Asp-138, O δ 2	2.73	0.68						
DEME	Asp-138, O δ 2	2.77	0.72	H ₂ O	3.03	0.89			
METH	Asp-138, O δ 2	2.67	0.57	H ₂ O	3.12	0.81			
GLCB	Asp-138, O δ 2	2.52	0.54						
O3 ALLO	Trp-99, N	3.01	0.85	Glu-297, O ϵ 1	3.03	0.47	H ₂ O	2.60	0.46
DEME	Trp-99, N	2.94	0.82				H ₂ O	2.77	0.78
METH	Trp-39, N	2.89	0.80						
GLCB	Trp-99, N	3.01	0.69				H ₂ O	2.90	0.87
O4 ALLO				Asn-100, N δ 2	2.93	0.43			
DEME							H ₂ O	2.63	0.92
METH				Asn-100, N δ 2	3.54	0.34			
GLCB									
O5 ALLO							H ₂ O	3.27	0.58
DEME									
METH									
GLCB									
O6 ALLO	Asp-213, O δ 2	2.49	0.71	H ₂ O + Asn-100, N	2.59,3.13	0.82,0.73	H ₂ O	3.21	0.31
DEME	Asp-213, O δ 2	2.58	0.76	H ₂ O + Asn-100, N	2.69,3.20	0.90,0.64	Glu-297, O ϵ 1, H ₂ O	2.42,2.64	0.60,0.60
METH	Asp-213, O δ 2	2.77	0.85	H ₂ O + Asn-100, N	2.89,3.22	0.81,0.79			
GLCB	Asp-13, O δ 2	2.83	0.69	Asn-100, N	3.02	0.87			
O7 ALLO	Tyr-212, O η	3.03	0.93	H ₂ O + Trp-358, N ϵ 1	2.90,2.67	0.62,0.58	Asn-100, N δ 2, H ₂ O	3.13,3.05	0.64,0.62
DEME	Tyr-212, O η	3.18	0.92	H ₂ O + Trp-358, N ϵ 1	2.88,2.66	0.69,0.53	Asn-100, N δ 2	2.43	0.42
METH	Tyr-212, O η	3.14	0.90	H ₂ O + Trp-358, N ϵ 1	3.10,2.64	0.62,0.44			
GLCB	Tyr-212, O η	2.99	0.98	Trp-358, N ϵ 1	2.67	0.56			

in binding upon removal of one of the methyl groups on the allosamidin moiety. The inhibition data of these derivatives on other chitinases (Table III) shows that there are two different classes: one that, similar to HCHT, shows a 10–100-fold drop for DEME compared with ALLO (the chitinases from *S. cerevisiae* and *C. albicans*) and another that does not show this effect (the chitinases from *Trichoderma harzianum* and *Bombyx mori*). In addition, HCHT and the chitinases from *T. harzianum* and *B. mori* bind ALLO 10–1000-fold better than the fungal chitinases from *S. cerevisiae* and *C. albicans*. Inspection of the HCHT·ALLO structure (Fig. 3) and a sequence alignment (Fig. 2) reveals two potential reasons for this difference in inhibition. First, the *S. cerevisiae* and *C. albicans* chitinases are similar to the relatively small plant chitinase hevamine, which lacks the extra $\alpha\beta$ domain that gives the active site a groove character and provides several contacts with the inhibitor (Tyr-267, Glu-297, and Met-300 in HCHT; Figs. 3 and 4). In addition, Met-210 and Met-356, two hydrophobic residues that form part of the pocket for the allosamidin methyl groups, are conserved in HCHT, *T. harzianum*, and *B. mori* chitinases but replaced by more hydrophilic residues in the small fungal chitinases.

Comparison of the Complexes—Despite the wealth of synthetic and natural allosamidins described in the literature, currently only complexes of family 18 chitinases with native ALLO have been determined (19, 20, 22). The complexes of HCHT with the DEME, METH, and GLCB allosamidin derivatives (Fig. 1) show no significant backbone conformational changes and superimpose with root mean square deviations of 0.32, 0.31, and 0.32 Å on HCHT C α atoms, respectively. Analysis of the binding pocket shows that although several key hydrogen bonds are conserved (Table IV and Fig. 3), there are differences in hydrogen bonding and side chain conformation.

Demethylallosamidin—In the HCHT·DEME structures, where the allosamidin lacks one of the methyl groups on the allosamidin (Fig. 1), the remaining methyl group points toward the oxygen side of the oxazoline ring, creating a small void that is filled by Glu-140 and Asp-138 rotating up to 30

degrees around $\chi_{1/2}$. This brings the Asp-138 O δ 2 atom closer to the allosamizoline nitrogen that carries the remaining methyl group, almost allowing formation of a hydrogen bond (distance 3.7 Å) (Fig. 3). This could explain the observed increase in affinity that is observed for DEME (Table III). There are no further noticeable conformational changes in the -1 binding site. The residues surrounding the allosamizoline moiety are the only ones that are highly conserved in family 18 chitinases (Figs. 2–4). Analysis of sequence differences does not reveal an amino acid change that is consistent with the different changes in inhibition when comparing ALLO and DEME binding to a range of chitinases (Table III). However, residues 95, 208, 210, and 356 do form part of the hydrophobic pocket for the allosamizoline methyl groups and are not conserved. It is possible that several concerted changes at these positions are responsible for the two types of effects on inhibition (*i.e.* no change or 10–100-fold stronger inhibition; Table III) for DEME.

Methylallosamidin—The structure of the HCHT-METH complex reveals that introduction of a methyl group on O6 of the -3 allosamine displaces an ordered water molecule from the binding pocket (Figs. 1 and 3). This ordered water molecule hydrogen bonds with DEME but not with ALLO (and is therefore not shown in Fig. 3-ALLO). In HCHT, addition of the methyl group to ALLO appears to increase the inhibition (Table III). A possible explanation could be the entropic gain through displacement of the ordered water molecule, yet a similar effect is not observed in the other chitinases (Table III). In the absence of structural data for these chitinases it is difficult to explain this, in particular because the entire α/β domain is missing in the smaller fungal chitinases (Fig. 2).

Glucallosamidin B—In the GLCB derivative three modifications are combined: removal of one of the allosamizoline methyls (as in DEME), addition of a methyl on O6 of the -3 allosamine (as in METH), and epimerization of the -2 allosamine to a glucosamine (Fig. 1). The HCHT-GLCB complex (Fig. 3) shows several changes compared with the HCHT-ALLO complex. In general, the GLCB molecule appears to be shifted about 0.5 Å toward the reducing end of the binding cleft (Fig. 3). This leads to weakening of the key hydrogen bonds in the -1 subsite (Table IV), which may be partially responsible for the weaker inhibition of HCHT, compared with the DEME and METH derivatives. Also, changes similar to those in the HCHT-DEME (rotation of Asp-138 and Glu-140) and the HCHT-METH complex (displacement of an ordered water molecule) are observed (Fig. 3). In addition, the equatorial O3 oxygen is no longer able to hydrogen bond another ordered water molecule observed in the HCHT-ALLO complex. The displacement of this water molecule leads to the loss of the water-mediated hydrogen bond with Arg-269 (Fig. 3). At the same time, however, the equatorial configuration of the O3 hydroxyl allows formation of the hydrogen bond with the pyranose oxygen of the -3 sugar, which is generally found in glucopolymers. The trends observed in the GLCB inhibition data (Table III) are similar to those for DEME, suggesting that removal of one of the allosamizoline methyls is the dominating effect.

Design of Specific Allosamidin Derivatives—Inhibition data of allosamidin and its derivatives show that there are significant differences in inhibition against the different chitinases (Table III). This suggests that if allosamidin is used as a template in novel synthetic studies aimed at designing derivatives against a specific chitinase, it would be possible to engineer a certain degree of specificity. This is important if such derivatives are used as antibiotics against human pathogens, as these molecules should not inhibit human chitinase, which has been

suggested to be part of an innate defense against chitinous pathogens (29–31). The structures described here allow for an evaluation of the potential for structure-based design of specific allosamidins. When sequence conservation is interpreted in the context of the HCHT-ALLO complex (Fig. 4) it appears that the only residues that are conserved and form part of the binding site are those interacting with the allosamizoline (Figs. 2–4). This would suggest it is difficult to make allosamizoline derivatives that are specific for certain chitinases. Yet not all residues contacting the allosamizoline are conserved (Fig. 2), and the differential inhibition for the DEME derivative (Table III) demonstrates it is possible to exploit these differences. For instance, Asn-100 makes hydrogen bonding interactions with the -2/-3 sugars (Fig. 3 and Table IV) yet is only present in the human chitinase. In general, there is no sequence conservation in the residues surrounding the -2 and -3 subsites (Figs. 2 and 4). This is especially true for the smaller *S. cerevisiae* and *C. albicans* chitinases, which lack the extra α/β domain that harbors several residues that are seen to interact with the allosamidins in the complexes described here (Figs. 2–4 and Table IV). Thus, the binding site in HCHT has a deep groove character, whereas in hevamine (and the closely related small fungal chitinases) it is a shallow pocket (22) (Fig. 4). Hence, it should be possible to design derivatives that have larger groups on the -2 and -3 sugars, fitting only the smaller, more open, chitinases. Alternatively, moieties could be introduced that interact specifically with side chains lining the deeper grooves of the larger chitinases.

Recently, an additional mammalian chitinase has been described that is mainly expressed in the stomach (29). This protein has 52% sequence identity with the human macrophage chitinase and also contains the additional α/β fold. Given the different expression patterns and the fact that this additional mammalian chitinase has a pH optimum of around 2, it is likely that it plays a different role than the human macrophage chitinase and has enough sequence differences to allow development of chitinase-specific inhibitors.

CONCLUSIONS

The structures of the human chitinase in complex with allosamidin and its derivatives have given new insights into the molecular mechanisms and specificity of these potent family 18 chitinase inhibitors. The dimethyl derivative, 10- to 100-fold more potent than allosamidin against most chitinases, appears to bind more strongly because of possible extra interactions with conserved residues that are part of the family 18 chitinase sequence signature. Modifications of the -2 and -3 *N*-acetylallosamines lead to displacement of ordered water molecules and altered hydrogen bonding with the protein. The structures could be used for further structure-based optimization of allosamidin.

Acknowledgments—We thank the European Synchrotron Radiation Facility (Grenoble) and the Deutsches Elektronen Synchrotron for the time at beamlines ID29 and X11, respectively. We also acknowledge Anneke Strijland, Jos Out, Ans Groener, and Marri Verhoek for technical assistance.

REFERENCES

- Kuranda, M. J., and Robbins, P. W. (1991) *J. Biol. Chem.* **266**, 19758–19767
- Wu, Y., Egerton, G., Underwood, A. P., Sakuda, S., and Bianco, A. E. (2001) *J. Biol. Chem.* **276**, 42557–42564
- Vinetz, J. M., Dave, S. K., Specht, C. A., Brameld, K. A., Xu, B., Hayward, R., and Fidock, D. A. (1999) *Proc. Natl. Acad. Sci. U. S. A.* **96**, 14061–14066
- Cohen, E. (1993) *Arch. Insect Biochem. Physiol.* **22**, 245–261
- Sakuda, S., Isogai, A., Matsumoto, S., Suzuki, A., and Koseki, K. (1986) *Tetrahedron Lett.* **27**, 2475–2478
- Kato, T., Shizuri, Y., Izumida, H., Yokoyama, A., and Endo, M. (1995) *Tetrahedron Lett.* **36**, 2133–2136
- Izumida, H., Imamura, N., and Sano, H. (1996) *J. Antibiot.* **49**, 76–80
- H. Izumida, M. Nishijima, T. T. A. N., and Sano, H. (1996) *J. Antibiot.* **49**, 829–831

9. Houston, D. R., Eggleston, I., Synstad, B., Eijnsink, V. G. H., and van Aalten, D. M. F. (2002) *Biochem. J.* **368**, 23–27
10. Shiomi, K., Arai, N., Iwai, Y., Turberg, A., Koelbl, H., and Omura, S. (2000) *Tetrahedron Lett.* **41**, 2141–2143
11. Arai, N., Shiomi, K., Yamaguchi, Y., Masuma, R., Iwai, Y., Turberg, A., Koelbl, H., and Omura, S. (2000) *Chem. Pharm. Bull.* **48**, 1442–1446
12. Houston, D. R., Shiomi, K., Arai, N., Omura, S., Peter, M. G., Turberg, A., Synstad, B., Eijnsink, V. G. H., and van Aalten, D. M. F. (2002) *Proc. Natl. Acad. Sci. U. S. A.* **99**, 9127–9132
13. Sakuda, S. (1996) in *Chitin Enzymology*, Vol. 2, pp. 203–212, Atec Edizioni, Grottammare, Italy
14. Bercibar, A., Grandjean, C., and Siriwardena, A. (1999) *Chem. Rev.* **99**, 779–844
15. Sakuda, S., Nishimoto, Y., Ohi, M., Watanabe, M., Takayama, S., Isogai, A., and Yamada, Y. (1990) *Agr. Biol. Chem. Tokyo* **54**, 1333–1335
16. Vinetz, J. M., Valenzuela, J. G., Specht, C. A., Aravind, L., Langer, R. C., Ribeiro, J. M. C., and Kaslow, D. C. (2000) *J. Biol. Chem.* **275**, 10331–10341
17. Tsai, Y.-L., Hayward, R. E., Langer, R. C., Fidock, D. A., and Vinetz, J. M. (2001) *Infect. Immun.* **69**, 4048–4054
18. Terwisscha van Scheltinga, A. C., Armand, S., Kalk, K. H., Isogai, A., Henrissat, B., and Dijkstra, B. W. (1995) *Biochemistry* **34**, 15619–15623
19. van Aalten, D. M. F., Komander, D., Synstad, B., Gåseidnes, S., Peter, M. G., and Eijnsink, V. G. H. (2001) *Proc. Natl. Acad. Sci. U. S. A.* **98**, 8979–8984
20. Bortone, K., Monzingo, A. F., Ernst, S., and Robertus, J. D. (2002) *J. Mol. Biol.* **320**, 293–302
21. Fusetti, F., von Moeller, H., Houston, D., Rozeboom, H. J., Dijkstra, B. W., Boot, R. G., Aerts, J. M. F., and van Aalten, D. M. F. (2002) *J. Biol. Chem.* **277**, 25537–25544
22. Terwisscha van Scheltinga, A. C., Kalk, K. H., Beintema, J. J., and Dijkstra, B. W. (1994) *Structure* **2**, 1181–1189
23. Vocadlo, D. J., Davies, G. J., Laine, R., and Withers, S. G. (2001) *Nature* **412**, 835–838
24. Tews, I., Terwisscha van Scheltinga, A. C., Perrakis, A., Wilson, K. S., and Dijkstra, B. W. (1997) *J. Am. Chem. Soc.* **119**, 7954–7959
25. Brameld, K. A., and Goddard, W. A. (1998) *J. Am. Chem. Soc.* **120**, 3571–3580
26. Hollak, C. E. M., van Weely, S., van Oers, M. H. J., and Aerts, J. M. F. G. (1994) *J. Clin. Invest.* **93**, 1288–1292
27. Renkema, G. H., Boot, R. G., Muijsers, A. O., Donker-Koopman, W. E., and Aerts, J. M. F. G. (1995) *J. Biol. Chem.* **270**, 2198–2202
28. Renkema, G. H., Boot, R. G., Strijland, A., Donker-Koopman, W. E., van den Berg, M., Muijsers, A. O., and Aerts, J. M. F. G. (1997) *Eur. J. Biochem.* **244**, 279–285
29. Boot, R. G., Blommaert, E. F. C., Swart, E., van der Vlugt, K. G., Bijl, N., Moe, C., Place, A., and Aerts, J. M. F. G. (2001) *J. Biol. Chem.* **276**, 6770–6778
30. Boot, R. G., Renkema, G. H., Verhoek, M., Strijland, A., Blik, J., de Meulemeester, T. M. A. M. O., Mannens, M. M. A. M., and Aerts, J. M. F. G. (1998) *J. Biol. Chem.* **273**, 25680–25685
31. Choi, E. H., Zimmerman, P. A., Foster, C. B., Zhu, S., Kumaraswami, V., Nutman, T. B., and Chanock, S. J. (2001) *Genes Immun.* **2**, 248–253
32. Otwinowski, Z., and Minor, W. (1997) *Methods Enzymol.* **276**, 307–326
33. Navaza, J. (1994) *Acta Crystallogr. Sect. A* **50**, 157–163
34. Brunger, A. T., Adams, P. D., Clore, G. M., Gros, P., Grosse-Kunstleve, R. W., Jiang, J.-S., Kuszewski, J., Nilges, M., Pannu, N. S., Read, R. J., Rice, L. M., Simonson, T., and Warren, G. L. (1998) *Acta Crystallogr. Sect. D Biol. Crystallogr.* **54**, 905–921
35. Jones, T. A., Zou, J. Y., Cowan, S. W., and Kjeldgaard, M. (1991) *Acta Crystallogr. Sect. A* **47**, 110–119
36. van Aalten, D. M. F., Bywater, R., Findlay, J. B. C., Hendlich, M., Hooft, R. W. W., and Vriend, G. (1996) *J. Comput. Aided Mol. Des.* **10**, 255–262
37. Laskowski, R. A., McArthur, M. W., Moss, D. S., and Thornton, J. M. (1993) *J. Appl. Crystallogr.* **26**, 283–291
38. Renkema, G. H. (1997) *Chitotriosidase, Studies on the Human Chitinase*. Ph.D. thesis, University of Amsterdam, Amsterdam, The Netherlands
39. Vriend, G. (1990) *J. Mol. Graph.* **8**, 52–56
40. Hooft, R. W. W., Sander, C., and Vriend, G. (1996) *Proteins* **26**, 363–376
41. Notredame, C., Higgins, D. G., and Heringa, J. (2000) *J. Mol. Biol.* **302**, 205–217

Crystal Structures of Allosamidin Derivatives in Complex with Human Macrophage Chitinase

Francesco V. Rao, Douglas R. Houston, Rolf G. Boot, Johannes M. F. G. Aerts, Shohei Sakuda and Daan M. F. Van Aalten

J. Biol. Chem. 2003, 278:20110-20116.

doi: 10.1074/jbc.M300362200 originally published online March 14, 2003

Access the most updated version of this article at doi: [10.1074/jbc.M300362200](https://doi.org/10.1074/jbc.M300362200)

Alerts:

- [When this article is cited](#)
- [When a correction for this article is posted](#)

[Click here](#) to choose from all of JBC's e-mail alerts

This article cites 37 references, 11 of which can be accessed free at <http://www.jbc.org/content/278/22/20110.full.html#ref-list-1>